PAPER • OPEN ACCESS

Heliosphere Configuration Insights from the Voyagers' Heliopause Crossings and Solar Disturbance Propagations

To cite this article: D S Intriligator *et al* 2020 *J. Phys.: Conf. Ser.* **1620** 012007

Heliosphere Configuration Insights from the Voyagers' Heliopause Crossings and Solar Disturbance Propagations

D S Intriligator[1], W D Miller[1], J Intriligator[1,2], and W Webber[3,4]
[1]Carmel Research Center, Inc., Santa Monica, CA
[2]Tufts University, Medford, MA
[3]New Mexico State University, Las Cruces, NM
[4]Deceased

E-mail: devriei@aol.com

Abstract. The Voyager 1 and 2 (V1 and V2) crossings of the heliopause (HP) have generated new estimates of the shape of the heliosphere, helped elucidate plasma wave features, and helped clarify particle and field phenomena, all of which provide insights into the overall configuration of the heliosphere and its interaction with the local interstellar medium (LISM). Webber and Intriligator (2011) suggested a consistent offset in the V1 and V2 locations of the termination shock (TS), predicted a shrunken and squashed geometry of the heliosphere, and correctly predicted that V1 would encounter the HP in 2012.0 ± 1 year. Intriligator et al. (2005, 2008) examined how the Halloween 2003 solar events were manifested from the Sun to V1 and V2 at 92.6 and 73.2 AU, giving rise to Global Merged Interaction Regions (GMIRs) and to broad particle, plasma, and magnetic field offsets that could affect the configuration of the heliosphere. The 2012 solar events (Intriligator et al., 2015) appeared to cause a tsunami at V1 and V2 at 128.7 and 102.5 AU and emphasized that space weather often could be interpreted as TS or HP or heliospheric crossings. Washimi et al. (2017) suggested that further complications of these events could propagate from the LISM back into the heliosphere. We conclude that in addition to the LISM magnetic field, the size and shape of the heliosphere are affected on differing time and space scales by changes in the average solar wind dynamic pressure over solar cycles with changing configurations of coronal holes, by pressure increases from GMIRs, and by magnetohydrodynamic instabilities that may be enhanced by energetic neutral atoms formed in GMIRs. We suggest the value of additional simulations that would combine our use of source surface maps of solar activity with other computational refinements.

1. Introduction

We honor the memory of Bill Webber (Figure 1) by recognizing his many significant predictions and energetic particle observations in space physics. Bill was a friend and inspiration worldwide to many researchers including at Carmel Research Center, Inc.

Figure 1. We are indebted to Bill Webber for his many important contributions, including predictions of phenomena that might be found within the heliosphere, beyond the heliopause, and analyses of Voyager and other spacecraft observations throughout these regions.

The size and shape, and their variations, of the heliosphere have long been the subjects of conjectures and theoretical models of how the solar wind (SW) and its embedded magnetic field (or for brevity, B field) form this vast bubble in the local interstellar medium (LISM). Now that both Voyagers have crossed the heliopause (HP) into the LISM from near the front of the heliosphere (as it moves through the LISM), and continue to return observations, it is possible to compare the measurements of plasma, B field, and energetic particle (i.e., cosmic ray systems (CRS) [1]) behavior from these and many other spacecraft with various conjectures and models.

The size and shape of the heliosphere are determined on various time and space scales by four major influences: the strength and orientation of the LISM B field; changes over the solar cycle of the magnitude and spatial dependence of the pressure of the SW with changing configurations of coronal holes; transient spatially dependent enhancements of the solar wind pressure by global merged interaction regions (GMIRs) generated by solar flares and other sources of coronal mass ejections (CMEs); and magnetohydrodynamic (MHD) instabilities in the SW-LISM interaction at the HP. The following sections describe available information about these influences and their effects.

2. Solar Wind Dynamic Pressures during Solar Cycles and the External B Field

Since shorter-term solar wind dynamic pressure variations relatively near the Sun, such as at 1 AU, smooth out as the SW moves outward and then decelerates at the TS in entering the heliosphere, Figure 2 shows two approaches to estimating the long-term dynamic pressure changes that influence the locations of the TS and the HP.

Figure 2(a) is from Webber and Intriligator [2] and shows how averages made from SWEPAM and OMNI data over Bartels solar rotations of 27 days for the years 1998 through 2010 (hence from before the peak of SC 23 through the SC 23-24 minimum) and smoothed by running averages of 5 rotations at a time showed a steep drop in dynamic pressure over the years 2004 through 2009. Allowing for travel time to and through the heliosheath and considering that V2 crossed the TS 10 AU closer to the Sun, at about 84 AU, than the V1 TS crossing at about 94 AU implied that by 2012, even though by then at the Sun SC 24 would be approaching its peak, the region within and near the HP should be shrunken and squashed, so that V1 was likely to reach the HP within a year of the beginning of 2012. This prediction of Webber and Intriligator [2] was fulfilled by the V1 HP crossing on August 25, 2012.

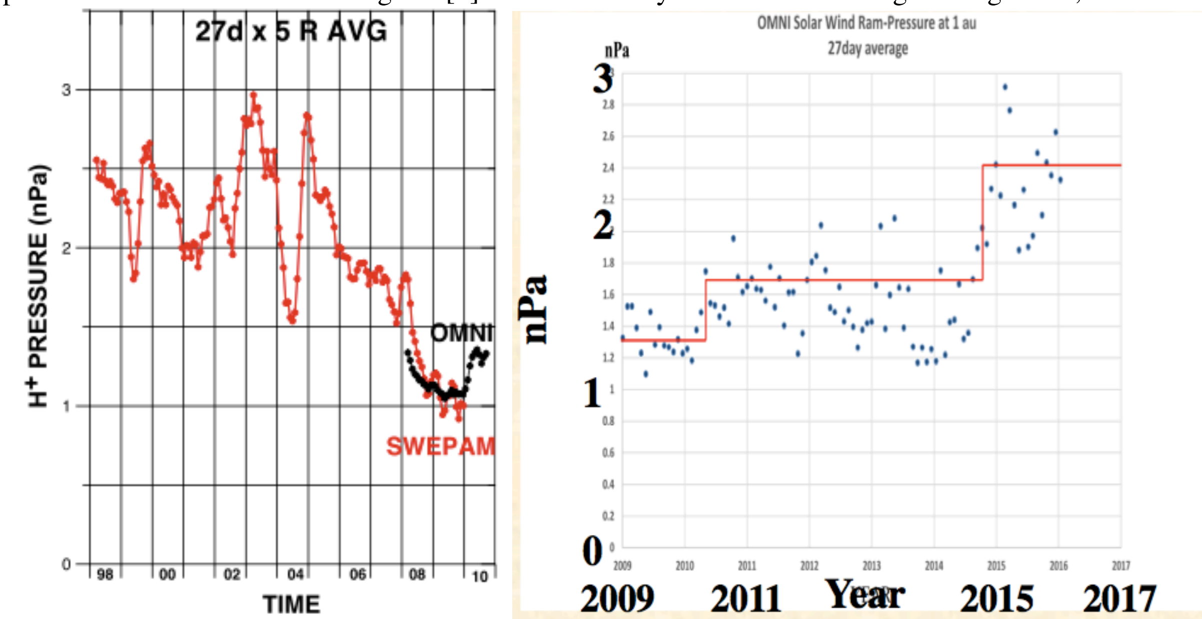

(a) (b)

Figure 2. Variations over solar cycles of the solar wind dynamic pressure near Earth. (a) Late SC 23: smoothed by running averages over 5 Bartels solar rotations (27-day periods) (Webber and Intriligator [2]). (b) SC 24: step function approximation to Bartels-rotation averages (Washimi et al. [3]).

Figure 2(b) is from Washimi, et al. [3] and uses 27-day averages of the OMNI data like those used for the black line in Figure 2(a). Webber and Intriligator smoothed the data. Washimi, et al. plotted the individual averages and then fitted a step function to them, for a cruder approximation to the long-term rise in dynamic pressure from the minimum in 2009 - 2010 through most of SC 24 to the beginning of 2016. (Note that the points for 2009 and 2010 at the beginning of this plot show the unsmoothed values that were used in the smoothed OMNI plot for 2009 and 2010 at the end of Figure 2(a).) This plot shows that by 2015 the ram or dynamic pressures had returned from the values below 1.5 nanopascals (nPa) that were typical during the solar cycle minimum to the values around 2.5 nPa that were typical around the peak of SC 23, as in Figure 2(a).

Figure 3 shows several hypothesized shapes that the heliosphere might have. It has long been recognized that if the LISM field were sufficiently weak then the heliosphere would resemble a comet, with the Sun and planets in the head and a tail stretching out many hundreds of AU downstream. Figure 3(a) shows a simulation by Pogorelov, et al. [4] based on this assumption, with the motion of the heliosphere from left to right in the figure, so that a bow wave of increased density builds up in the LISM ahead of the forward HP and the tail extends about 2000 AU downstream. The stripes in the tail in this figure are regions of alternating B field produced by successive solar cycles, so that the farthest parts of the tail consist of SW emitted more than a century earlier and the whole tail is based on exact repetitions of an idealized solar cycle of conditions at 1 AU.

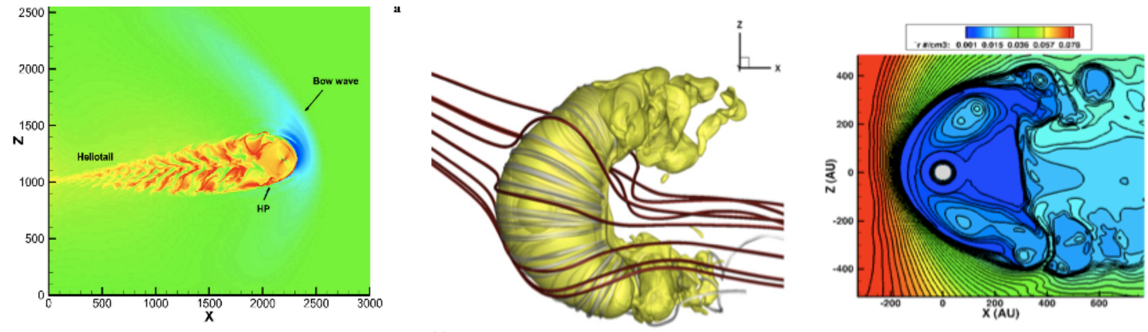

(a) (b) (c)

Figure 3. Hypothesized heliosphere shapes. (a) Extremely long cometary shape in a weak LISM magnetic (B) field. Stripes are alternating field regions due to solar cycles [4]. (b) “Croissant” shape in a stronger LISM B field. Polar jets are bent by motion through the LISM, with the LISM B field producing turbulent mixing and energetic neutral atoms (ENAs) [5]. (c) More nearly spherical shape for which polar jets pinch off closer to the Sun than in the “croissant” model. Colors show combined density of SW and Pick Up Ion (PUI) plasma in cm^{-3} in the meridional plane. [6]

However, the B field measurements in the LISM from V1 and V2, combined with ENA data from Cassini and IBEX now indicate (Dialynas, et al., [7]) that the field is likely to be too strong for the cometary shape, so Figure 3 also shows two possible configurations for this case. Figure 3(b) depicts the HP as it might be if the heliosphere were moving from right to left past a viewpoint located outside, with the lines of the LISM field wrapping around the heliosphere at low and medium solar latitudes and curving irregularly in a turbulent downstream region, while solar wind jets from polar coronal holes extend the higher latitudes of the heliosphere far enough to be bent into a croissant-like shape by the motion through the LISM (Opher, et al., [5]). The points of the “croissant” then pinch off irregularly in a turbulent interaction with the LISM, so the solar wind plasma mixes with the LISM plasma and neutral gas in a way that produces numerous ENAs, providing an alternative reason for the enhanced fluxes of ENAs observed by IBEX from higher latitudes in the downstream direction reported by McComas, et al. [8]. They interpreted the sources of these ENAS to be lobes in the tail of a cometary configuration like that in Figure 3(a).

Figure 3(c) shows a modification of the “croissant” concept (Opher, et al., [6]) in which the polar jets pinch off at smaller distances to produce a more nearly spherical heliosphere, but the turbulent mixing still generates ENAs observed at higher latitudes. This figure is a meridional section through a simulation of the heliosphere in which it is also moving from right to left, and the colors indicate the combined density of SW and PUIs. Thus, the heliosphere density is relatively low and there is a region of much higher density ahead in the LISM, analogous to the bow wave depicted in Figure 3(a).

In a manner somewhat analogous to the depiction in Figure 2 of the changing solar wind dynamic pressure near the solar equator over the solar cycle, the changing configuration of coronal holes over the solar cycle implies substantial changes in the solar wind dynamic pressure at higher latitudes, raising the possibility that the shape of the heliosphere may shift over a solar cycle between a configuration like that in Figure 3(b) and one like Figure 3(c) and back again.

This is suggested by the way that large coronal holes cover the poles of the Sun during solar minimum, but around solar maximum the polar field lines are mostly closed, as depicted in Figures 4 and 5, and also indicated by Ulysses solar wind observations during its polar orbits near the SC 22 - 23 minimum, near the SC 23 maximum, and near the SC 23 - 24 minimum (Intriligator, et al. [9]).

Figure 4 shows two examples of one type of display of the field and coronal holes that the National Solar Observatory (NSO) Integrated Synoptic Monitoring Program (NISP) [10] derives from solar magnetograph observations. Figure 4(a) is the image for Carrington Rotation (CR) 2048, from late September, 2006, through most of October, 2006, near the SC 23 - 24 minimum, while Figure 4(b) is the image for CR 2139, from early July, 2013, through early August, 2013, near the SC 24 maximum.

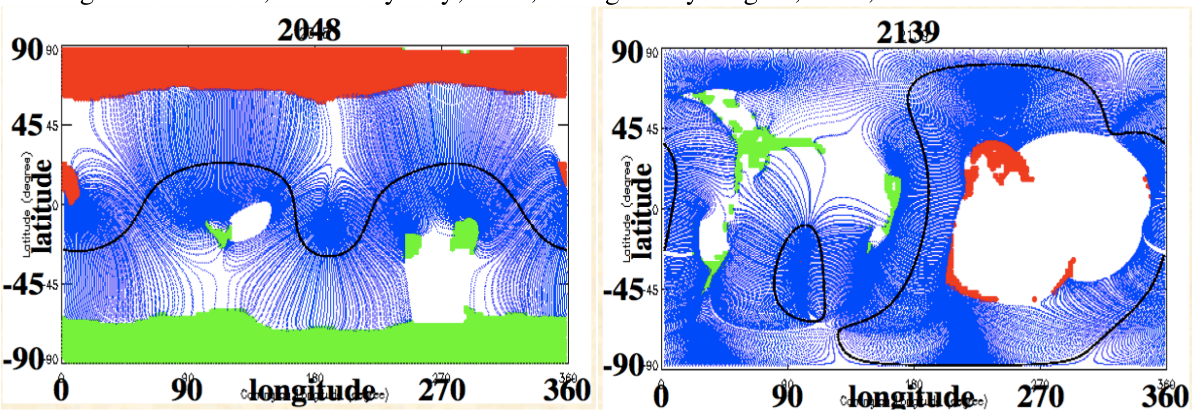

(a) (b)

Figure 4. Mercator displays of actual coronal holes and closed solar field lines during example CRs of SC 24. Red: B field inward; Green: B field outward; Thin blue lines: closed field lines; Black line: base of the HCS. Horizontal axes are Carrington longitudes. (a) Solar minimum: CR 2048, 9/21/2006 - 10/19/2006. ([10], 2006) (b) Solar maximum: CR 2139, 7/8/2013 - 8/5/2013. ([10], 2013)

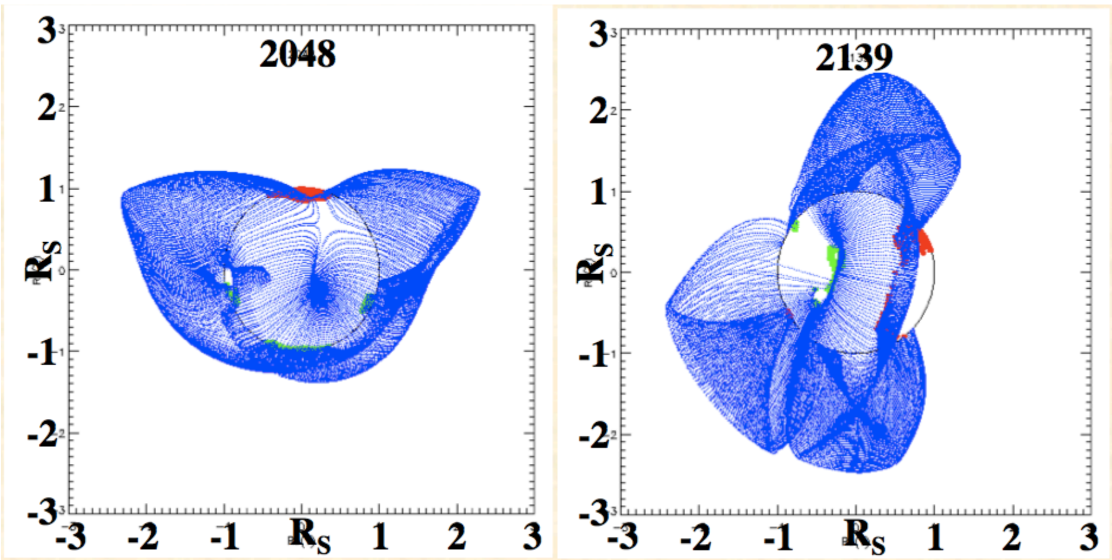

(a) (b)

Figure 5. Perspective views, with the same colors, of the solar fields shown in Figure 4, for coronal holes during SC 24. All axes are in solar radii. (a) CR 2048. (b) CR 2139. ([10], 2006, 2013)

The depictions in Figure 4 in latitude and Carrington longitude are analogous to Mercator projections of the terrestrial globe, and therefore overemphasize regions at higher latitudes, so Figure 5 shows the perspective views of the magnetic field for CR 2048 and 2139 also provided by the NISP. These views are in solar radii instead of in the latitude and Carrington longitude of Figure 4 and are centered on longitude 180 of the Mercator views, so they provide a clearer view of the geometry at higher latitudes of the holes and field lines near longitude 180 but obscure everything at longitudes less than 90 and greater than 270. Thus, Figure 5(a) clearly shows the large north polar coronal hole, although the similar one at the south pole is much harder to see, while Figure 5(b) is a vivid depiction of both poles being covered by closed field lines. Then comparing this with Figure 4(b) shows how the base of the HCS extends almost exactly from one pole to the other. Hence, allowing for delays, the changing latitudinal distribution of solar wind dynamic pressure could produce a heliospheric shape that was shrunken and squashed at low and medium latitudes (recall that V1 is near 34 N and V2 is near 32 S) but extended at higher latitudes, as in Figure 3(b), when the solar wind emitted near solar minimum approaches the HP, while the solar wind emitted near solar maximum would be expected to let the heliosphere shrink at higher latitudes while pushing it out more at lower latitudes (especially downstream, away from the dynamic pressure of plowing through the LISM), as in Figure 3(c).

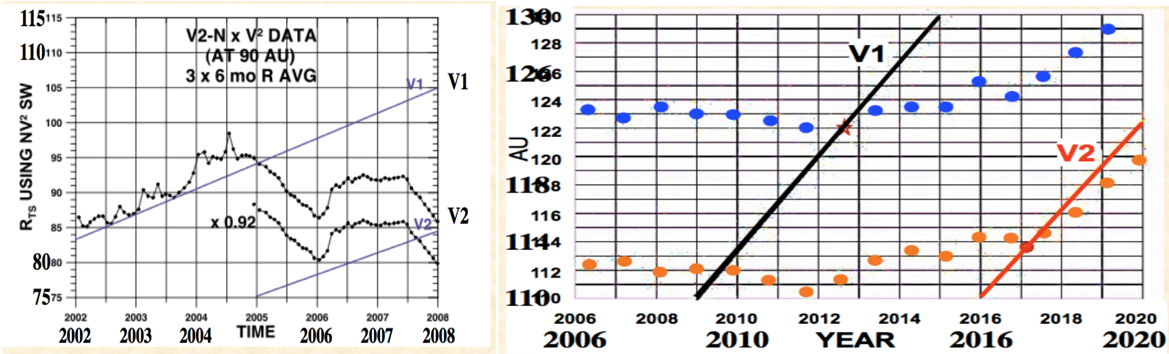

(a) (b)

Figure 6. Estimated variations of the TS and HP distances along the trajectories of V1 and V2 due to solar wind pressure changes as the spacecraft were approaching these boundaries. (a) TS distances 2002 - 2008 (Webber & Intriligator [2]). (b) HP distances 2006 - 2020. Blue dots are for V1; orange dots are for V2, predicting an HP crossing early in 2017 (Washimi et al. [3]).

Figure 6 shows the estimated variations of the TS and HP positions for V1 and V2 based on the pressure change averaging in the graphs in Figure 2. Figure 6(a), from [2], shows estimated locations of the TS for V1 and V2 during 2002 through 2007, indicating that V1 came close to the TS several times in 2002 and 2003 as it was moving outward but never actually crossed until the end of 2004, when the TS had begun to move inward. Likewise, V2 crossed at the end of August and the beginning of September of 2007, as the TS was moving inward. Similarly, Figure 6(b) shows that Washimi et al. [3] concluded that V1 crossed the HP at a time when it was relatively close to the Sun, just before it would have begun moving outward again, while their calculation predicted that V2 would cross in early 2017, just as the HP was starting to move outward. As described in the next section, we suggest that taking into account the transient effects of MIRs generated by solar flares provides a possible explanation why the actual V2 HP crossing did not occur until late 2018.

3. Transient Effects of MIRs

Many years of observations and analyses have shown that when solar flares and other sources of CMEs produce shocks that pass the Earth separately but at intervals of a few hours or a few days, the later ones tend to catch up with the earlier ones as they move outward through the solar system, so that the resulting global merged interaction regions (GMIRs) are an important feature of the space environment around the outer planets and beyond them. As we and many other authors have discussed (e.g., Intriligator, et al. [9,11]), plasma wave events observed by the V1 PWS around 3 kHz [12] have shown that GMIRs generated by the most powerful sequences of flares in recent years have propagated out through the heliosphere into the region of the LISM around the trajectory of V1.

On the other hand, as flares (and less violent sources of CMEs, such as collapsing helmet streamers, to the extent that such events may contribute to MIRs that reach the LISM) are highly localized on the Sun, the MIRs they generate are asymmetrical, so that their effects on the size and shape of the heliosphere are not only transient but dependent on the locations of the source events.

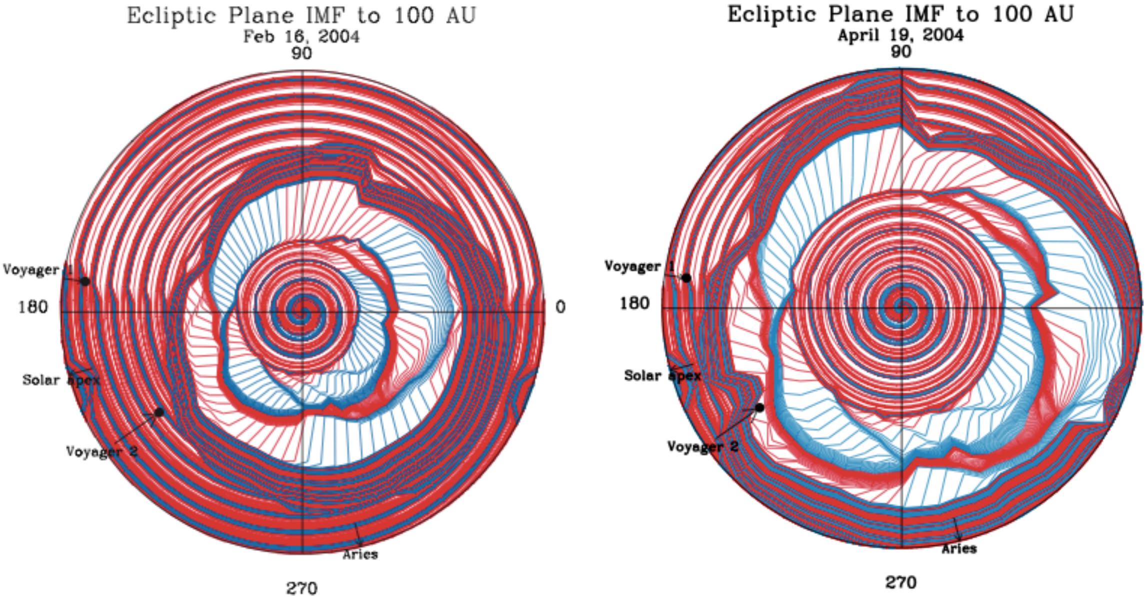

(a) (b)

Figure 7. HAFv2 calculation of large-scale effects on the Ecliptic plane IMF of the Halloween 2003 events. Red: B field outward; Blue: B field inward. (a) February 16, 2004. (b) April 19, 2004. [13]

Thus, for example, for the "Halloween 2003 events," which were a sequence of flares that occurred in October and early November of 2003, including several notably powerful ones within a few days of Halloween, Figure 7 shows two stages of the expansion of the MIR that they generated, according to the HAFv2 model of Intriligator, et al. [13]. (Note that since neither V1 nor V2 had reached the TS at the time of this computation, no estimate of its location was included in the model.)

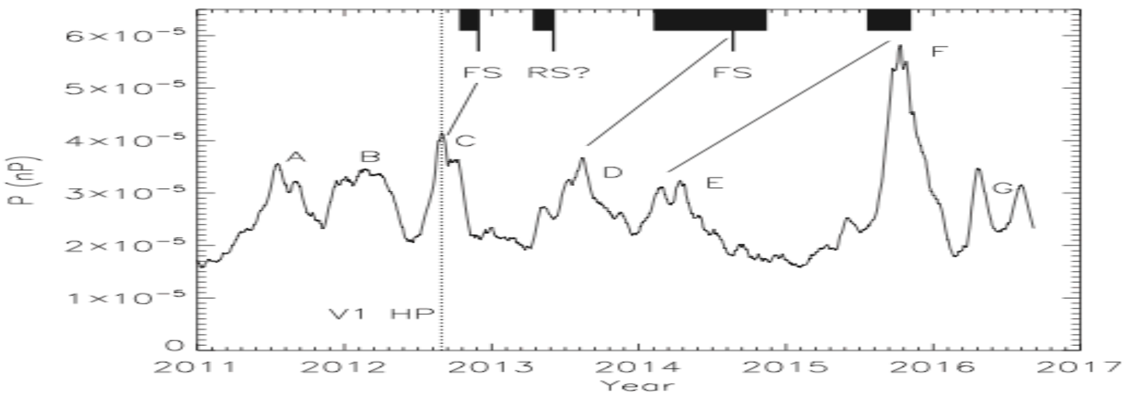

Figure 8. Dynamic pressure variations at V2, 2011 - 2017. Peaks C - F were identified as MIRs. [14]

In view of this evidence for the importance but also the complexity of the effects of MIRs, it is likely that the dynamic pressure variations observed at V2 that are shown in Figure 8 (Richardson, et al. [14]) pushed the HP around the trajectory of V2 farther out into the LISM than it would have been if they had not occurred, but in the absence of more detailed modeling it is not possible to reliably extrapolate their effects away from the trajectory of V2.

Thus, Figure 9 shows how the pressure peaks in Figure 8 might have modified the locations in Figure 6(b) of the HP along the trajectory of V2 from Washimi, et al. [3], but does not attempt corresponding estimates of how the MIRs that produced these peaks might have changed these authors' locations of the HP along the trajectory of V1. (Also, any such estimates would be irrelevant, since V1 had already crossed the HP.) Hypothesizing that the approximately equal-sized peaks A - E each added 0.2 AU to the distance of the HP, that the much larger peak F added 0.5 AU, and that the tiny pair of peaks at G had no effect produces the green line in Figure 8. In two ways this improves the agreement between the V2 observations and the revised HP locations, compared to the original ones.

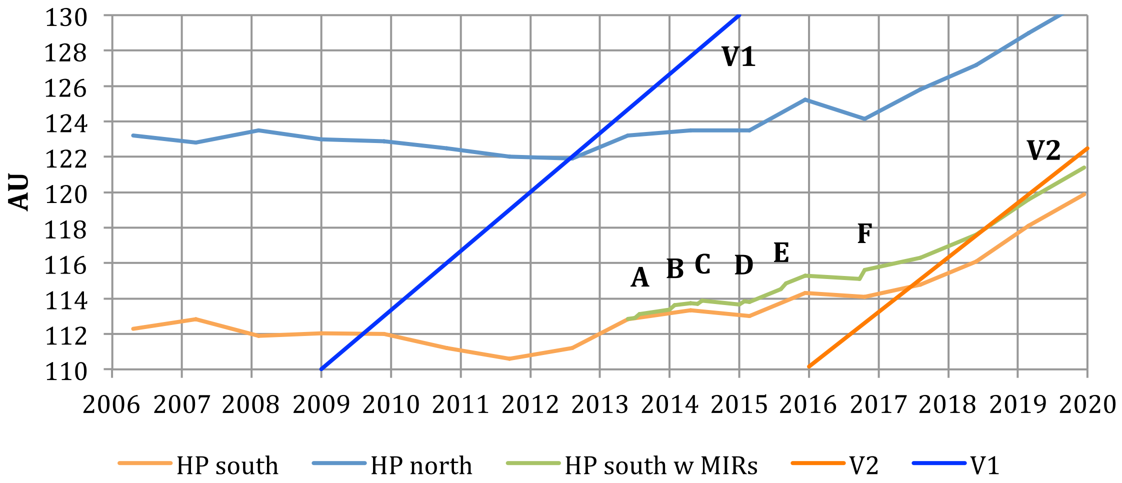

Figure 9. Modification of Figure 6(b), showing a possible effect of pressure peaks A - F in Figure 8 on the location of the HP for V2. The green line shows the effect if peaks A - E each move the HP 0.2 AU farther out and F moves it 0.5 AU farther out, resulting in a predicted HP crossing much closer to the actual time in November, 2018. Blue and orange lines are the same as in Figure 6(b) from [3].

First, we point out that it postpones the predicted time of the HP crossing to the middle of 2018, much closer to the actual time in November. Second, the HP is depicted as moving outward nearly as fast as V2, resulting in a slower relative speed of approach than is implied by the orange line of Washimi, et al.'s estimates. This agrees with the observed way that the period between the first indications of approaching the HP and the actual crossing was much longer for V2 than the corresponding period for V1. (Some analyses of the V2 observations around its HP crossing (e.g., Burlaga, et al. [15]) have assumed a stationary HP, hence implying a much thicker transition region than along the V1 trajectory, but as described in Section 2, considering the long-term changes in average solar wind pressure over solar cycles provides a persuasive reason why the HP should move.)

4. A Possible Effect of MIRs on MHD Instabilities at the HP

As we have noted before (Intriligator, et al. [11]), the HP is expected to show various fluctuations and irregularities due to MHD instabilities, with the Rayleigh-Taylor instability occurring in the region of the nose of the heliosphere and the Kelvin-Helmholtz instability along the flanks. The count rates from the CRS instruments [1] on V1 and V2 in Figure 10 exemplify not only possible effects of these instabilities but also the difficulty of characterizing these effects from isolated observation points.

Figure 10(a) shows the count rates from the V1 CRS for galactic cosmic rays (GCRs), with energies >70 MeV, and for particles with energies >0.5 MeV. These of course include the GCRs, but in the region inside the HP and just beyond it the count rates in this energy interval result mostly from solar cosmic rays and anomalous cosmic rays (ACRs), all of which have energies >0.5 MeV and <70 MeV and may collectively be designated as solar system cosmic rays (SSCRs). The blue stars indicate the well-known five HP crossings that occurred as the spacecraft was leaving the heliosphere, which are obvious evidence of unstable behavior at the HP. The two pairs of crossings before the final one have been interpreted as crossings of flux tubes of LISM that had penetrated the outer edge of the heliosphere, but the second pair of crossings, between days 225 and 230 lacks the neat symmetry of the first pair, both in the particle count data and in the magnetometer readings (not shown), raising the possibility that these crossings merely resulted from fluctuations in the HP, analogous to the fluctuations in the TS that probably caused the five crossings of that shock that V2 observed in 2007.

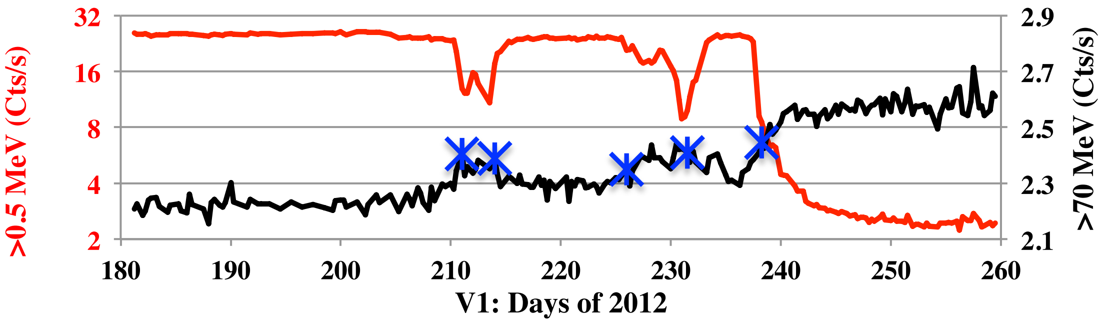

Figure 10(a). V1 HP-epoch particle count rates. Red: SSCR (>0.5 MeV, left axis); Black: GCR (>70 MeV, right axis); Blue stars: HP crossings. [1]

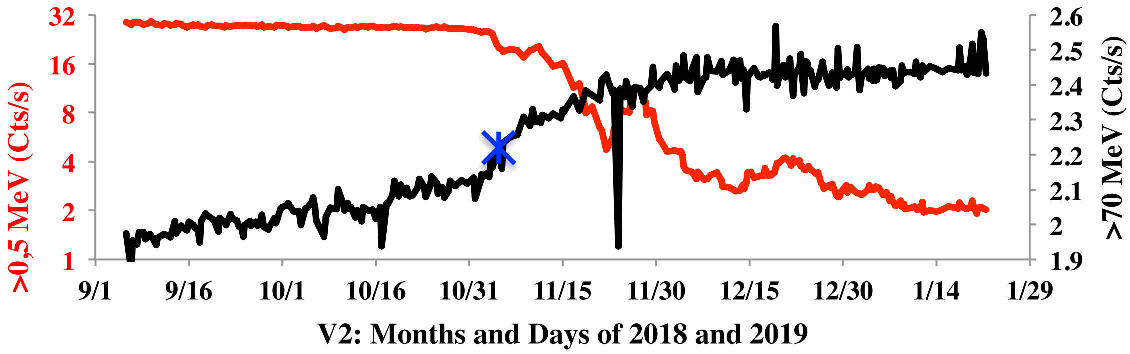

Figure 10(b). V2 HP-epoch particle count rates. Red: SSCR (>0.5 MeV, left axis); Black: GCR (>70 MeV, right axis); Blue star: HP crossing. [1]

Since the SSCR count rate declined steeply at V1 after the last HP crossing, and since (as described in more detail in Intriligator, et al. [16]) this is likely to be due to the effect of the LISM plasma flow sweeping away SSCRs that cross the HP, the irregularities in the decline of the SSCR count rate in the V2 CRS shown in Figure 10(b) after this spacecraft's single HP crossing strongly suggest that the location of the HP fluctuated enough to bring it closer to the spacecraft at least twice in the last weeks of 2018, without catching up with it.

Furthermore, in addition to the effects of the pressure enhancements produced by MIRs that were discussed in Section 3, Borovikov, et al. [17] describe how it is likely that MIRs generate enhanced fluxes of ENAs that transiently enhance the instabilities at the HP.

They pointed out that there are two distinct populations of outflowing ENAs produced from the SW by charge exchange with inflowing interstellar neutral gas, since ENAs formed from the SW in the supersonic region move radially at about 400 km/s, while ENAs formed from the subsonic SW beyond the TS have speeds of about 150 km/s and directions determined by the deflection of the subsonic SW from radial flow. Portions of each of these ENA populations then undergo charge exchange with ions in the LISM, forming populations of PUIs that increase the plasma beta around the HP and thereby contribute to the instabilities. As the fast ENAs would form PUIs with a higher effective temperature, each of them would contribute more to the plasma beta than a corresponding slow ENA.

As the rate of formation of ENAs from the SW increases with the SW density, and since the pressure increases in MIRs primarily are density increases, this reasoning implies (though the Voyagers had no ENA instruments, so that no observations are available to confirm the reasoning) that as a MIR travels outward in the supersonic region it would form a region of higher density of fast ENAs that would accompany it until it decelerated at the TS. Then they would continue on while the MIR moved subsonically through the heliosheath, building a region of higher density of slow ENAs that would accompany it until it reached the HP.

Thus, at the HP each MIR would be expected to be preceded by a burst of fast ENAs, arriving several months before the MIR and the slower ENAs, but each burst would enhance the instabilities, producing wrinkles and ripples and perhaps more complex fluctuations in the region of the HP where the ENAs emerged. Then the asymmetry of MIRs noted in Section 3 would be a further source of transient irregularities in the shape of the heliosphere, as the ENAs emerged in different regions.

5. Modeling

The observations and analyses discussed in the preceding sections suggest two conclusions. One is that since the Voyagers have now crossed the HP and the only other spacecraft currently recording in-situ observations of the outer solar system is New Horizons (which like the Voyagers is traveling toward the nose of the heliosphere, but has a trajectory near the solar equator, in contrast to the northerly and southerly trajectories of V1 and V2, respectively), for the foreseeable future the only source of additional insight into many questions about the structure and behavior of the heliosphere will be modeling. The second is that the various modeling studies that we have cited in this and previous discussions (e.g., Intriligator et al., [9,16]) including both those by Carmel Research Center and those by others, show the great challenges confronting an effort to construct models that would incorporate the many phenomena that are now known to be relevant.

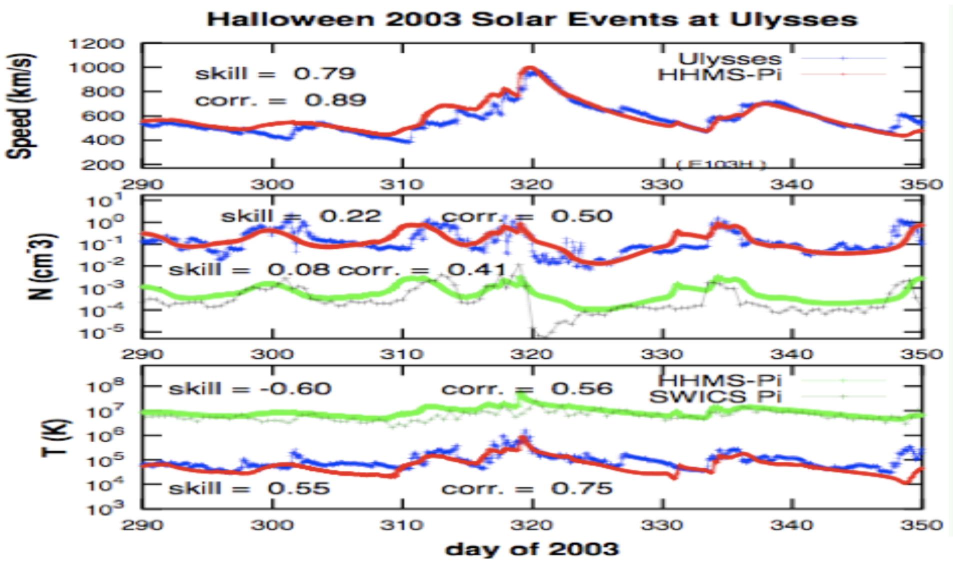

Figure 11. Comparisons between HHMS-PI simulation values (red and green lines) and Ulysses SWOOPS solar wind observations (blue lines) and SWICS PI observations (faint gray lines) [19].

For example, Figure 11, from Intriligator et al. [19] is an example of good agreement between Ulysses observations of the effects of the Halloween 2003 events (mentioned above in Section 3) and a MHD model that used inputs from the Wang-Sheeley-Arge (WSA) source surface maps and incorporated the effects of inflowing neutral gas forming pickup ions. Intriligator et al [19] discussed the ENA models disagreement with the PUI measurements in the N (cm-3) density panel near Day 320. They suggested that this could have been caused by ENA interactions. Previously Intriligator et al. [20] showed that the magnetic structure of these events was caused by planar magnetic structures in the SW. The same modeling methodology succeeded in reproducing many observations of the space weather "tsunami" generated by the great flare of 23 July 2012 [21]. However, the computation method in this program was specific to supersonic flow conditions, so that code for another method would need to be added to describe the subsonic conditions beyond the TS. Likewise, although the model formulas included terms for formation of pickup ions from neutral gas, there was nothing to describe the formation of fast outflowing ENAs.

On the other hand, Figure 12 shows that ENA effects were successfully incorporated into a simulation done with HAFSS, which is a revision of the HAFv2 program that produced the MIR propagation simulations in Figure 7. In Figure 12 the simulated shape on the right agrees well with the shape of the actual IBEX Ribbon on the left, but the simulation greatly overestimated the count rates.

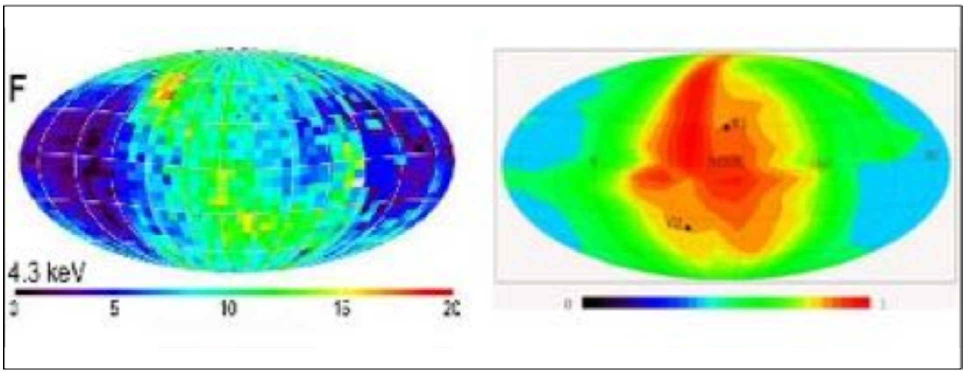

Figure 12. HAFSS simulation of IBEX data [18], showing qualitative prediction of the IBEX Ribbon.

The best hope for improved modeling may be to combine the use of inputs from WSA source surface maps (as in HHMS-PI, HAFv2, and HAFSS, but not in other modeling studies of which we know) with other refinements (i.e., as in Pogorelov, et al. [4]), and numerous other simulation studies).

A sufficiently comprehensive simulation might resolve other questions about heliospheric phenomena, such as testing theories that ACRs are accelerated at the TS at longitudes that are farther along the flanks of the heliosphere than the Voyager trajectories, since during their TS crossings neither V1 nor V2 observed ACR acceleration in the way that had been expected. Perhaps it will also be possible to gain additional insight into other phenomena that have not been observed from spacecraft and are not likely to be observed for many years, such as the interaction of the interplanetary B field and HCS with the particles and fields of the LISM when the HCS extends to high latitudes around solar maximum, which Figures 3(b) and 3(c) suggest may have complexities deserving additional attention.

This consideration is an example of the eventual need for simulations to extend in some way beyond the HP. Understanding the IBEX Ribbon better is one obvious goal, but there are others. In Intriligator, et al. [16] we proposed that the excess Lyman α radiation observed by the V1 UV spectrometer (Katushkina, et al. [22]) and the Alice UV spectrograph on New Horizons (Gladstone, et al., [23]) results from charge exchanges in the LISM that are sufficiently energetic to produce excited hydrogen atoms, but we did not consider the possible effect of energetic neutral hydrogen atoms that would be generated in the heliosphere by the MIR, as discussed in Section 4. (Note that the fast ENAs generated in the supersonic region would also differ between those generated from the slower equatorial SW and those from fast coronal hole SW.) We also did not consider possible effects of ions of heavier elements from the SW in the LISM. Another topic that appears to deserve better understanding is the role played by plasma ions and electrons in the conversion of magnetosonic turbulence into incompressible turbulence in the LISM reported by Burlaga, et al. [24] and discussed further by Zank, et al. [25], in which the Kolmogorov spectrum is preserved in the conversion to Alfven waves. These examples indicate the potential importance of developing better simulation methods for LISM processes and connecting them to simulations within the heliosphere.

6. Concluding Remarks

From comparing and analyzing a wide range of observations and events, including the ones discussed in the preceding sections, we conclude that in addition to the LISM magnetic field, and to the size and shape of the heliosphere, all are affected on differing time and space scales by changes in the average solar wind dynamic pressure over solar cycles with changing configurations of coronal holes, by pressure increases from GMIRs, and by MHD instabilities that may be enhanced by ENAs formed in GMIRs. We recommend more modeling to use solar activity source surface maps with other refinements of previous computational methods.

This is particularly true because there are few heliophysics measurements for comparison where Ulysses was (as shown in Figure 11) and even fewer farther out in the heliosphere, the heliosheath, and beyond the HP in the LISM. New Horizons is making heliospheric observations far from the Sun. The Voyagers are farther out and probably have only a few more years to operate in the LISM. Thus, more detailed understanding of past as well as future in-situ observations and of remote observations of regions where spacecraft have never gone is most likely to come from increased realism in modeling. We have always sought to use the best available information about the activity of the solar source of the interplanetary medium, as well as developing increasingly realistic descriptions of transport phenomena and of interactions with the plasma and neutral components of the LISM. We believe that developing this approach further will lead to new important understanding.

Astronomers have catalogued many stars that are in spectral class G, and are quite similar to the Sun, so they may have astrospheres like the heliosphere. Many are now known to have planets. Some are observed to have Sun-like activity cycles. The Sun and its activity and the heliosphere are close enough to be observed in detail in ways that will never be possible for the analogous more distant objects and phenomena, so that everything that we can learn about the heliosphere and its contents not only has local significance but contributes to understanding vast regions of the universe beyond.

Acknowledgments

We thank the V1 and V2 projects for their vast observations, including the CRS [1]. plasma [13], magnetic field [15], and PWS [12] data. We are grateful for Ulysses SWOOPS from McComas [8] and SWICS from the Gloecklers [19]. We acknowledge the support of Carmel Research Center, Inc. We acknowledge Professor Gary Zank and Adele Corona for these excellent conferences and papers.

7. References

[1] CRS homepage: https://voyager.gsfc.nasa.gov; rates: https://voyager.gsfc.nasa.gov/rates.html
[2] Webber W R and Intriligator D S 2011 *J. Geophys. Res.* **116** A06105
[3] Washimi H *et al.* 2017 *Astrophys. J. Lett.* **846** L9
[4] Pogorelov N *et al.* 2017 *Astrophys. J.* **845** 9
[5] Opher M *et al.* 2015 *Astrophys. J. Lett.* **800** L28
[6] Opher M *et al* 2019 ArXiv 1808.06611
[7] Dialynas K *et al.* 2019 *Geophys. Res. Lett.* **46** 7911
[8] McComas D J *et al.* 2013 *Astrophys. J.* **771** 77
[9] Intriligator D S *et al.* 2017 *16th AIAC J. of Phys. Conf. Ser.* **900** 105
[10] NSO Integrated Synoptic Program (NISP) Integral PFSS model synoptic coronal hole plot http://gong2.nso.edu/archive/patch.pl?menutype=z
[11] Intriligator D S *et al.* 2018 *17th AIAC J. of Phys. Conf. Ser.* **1100** 012013
[12] Gurnett D A *et al* 2015 *Astrophys. J.* **809** 121
[13] Intriligator D S *et al.* 2005 *J. Geophys. Res.* **110** A09S10
[14] Richardson J D *et al.* 2017 *Astrophys. J.* **834** 190
[15] Burlaga L F *et al.* 2019 *Nat. Astron.* **3** 1007
[16] Intriligator D S *et al.* 2019 *18th AIAC J. of Phys. Conf. Ser.* **1332** 012006
[17] Borovikov S *et al.* 2008 *Astrophys. J.* **682** 1404
[18] Intriligator D S *et al.* 2016 *15th AIAC "The Science of Ed Stone Celebrating his 80th Birthday:" Journal of Physics Conference Series* **761** 012013
[19] Intriligator D S *et al.* 2012 *J. Geophys. Res.* **117** A06104
[20] Intriligator D S *et al.* 2008 *J. Geophys. Res.* **113** A05102
[21] Intriligator D S *et al.* 2015 *J. Geophys. Res.* **120** 8267
[22] Katushkina O A *et al.* 2017 *J. Geophys. Res.* **122** 10921
[23] Gladstone G R *et al.* 2018 *Geophys. Res. Lett.* **45** 8022
[24] Burlaga L F *et al.* 2018 *Astrophys. J.* **854** 20
[25] Zank G P *et al.* 2019 *Astrophys. J.* **887** 116